The Structure and Molecular Packing of the ω Form of Poly(β-benzyl L-aspartate) Electron Diffraction Studies

J. P. Baldwin,* E. M. Bradbury, I. F. McLuckie, and R. M. Stephens

Biophysics Laboratories, Physics Department, Portsmouth Polytechnic, Portsmouth PO12DZ, England. *Received July 17, 1972*

ABSTRACT: After heating thin films of *both* the left- and right-handed α-helical-like forms of poly(β-benzyl L-aspartate), ω-helix electron diffraction patterns are observed which confirm the earlier X-ray diffraction data of Bradbury *et al.* A model is proposed where the ω helices are packed parallel within thin lamellae with helices in adjacent lamellae antiparallel and shifted sideways by half-lattice spacing. The atomic coordinates proposed earlier by Bradbury *et al.* agreed with deductions from infrared dichrosim measurements, and if these are rotated 5° anticlockwise in the unit cell and used with the above lamella model they predict the observed absence of (110) and (330) diffraction spots. They also predict equatorial diffraction intensities in somewhat better agreement with observed intensities than would a model with a random distribution of parallel and antiparallel helices. The model predicts intensities on the first-layer line in quite good agreement with the observations when the antiparallel helices are displaced $\sim+5c/16$ relative to the parallel helices and satisfactory Van der Waals interactions between the lamellae occur with the above atomic coordinates. Meridional reflections (001), (002), and (003) which should be absent for a perfectly helical structure are accounted for by distortions in the atomic positions for residues associated with interactions between antiparallel helices.

Solid films of poly(β-benzyl L-aspartate), $(BzAsp)_n$, can be prepared either as a left-handed α-like helix[1,2] when cast from chloroform solution, or as a right-handed α-like helix when prepared by the monolayer techniques used by Malcolm.[3,4] The X-ray and electron diffraction patterns of both these forms are poorly defined.

By heating solid films of the α forms of both helix senses to temperatures of the order of 140°, a phase change to a highly ordered structure occurs. Bradbury *et al.*[5] have shown that the molecules in this structure form 4_{13} helices, the ω helix, of the type described earlier by Bragg, Kendrew, and Perutz.[6] In this structure for $(BzAsp)_n$ there are four residues per turn of the helix and the helices are tetragonally packed. Malcolm[4] and McLuckie[7] have noted that closely similar *d* spacings occur whichever sense α-like helix is heated to form the ω structure.

Detailed infrared dichroism studies of the ω helix in the polypeptide[5,8,9] have established the orientations of many of the bonds in the side chains, and X-ray diffraction analysis with model building by Bradbury *et al.*[5] has yielded proposed atomic coordinates for the structure in good agreement with the infrared data and with a space group assignation $P4_3$.

The above work[5,9] showed that part of the energy for the ω-helix structure in $(BzAsp)_n$ was derived from intramolecular van der Waals interactions which lead to a stacking of the benzene rings in the residues with each fifth residue being stacked directly above a chosen first residue. However, it was clear that intermolecular interactions must also be important in determining the minimum energy structure since the ω structure occurs only in solid $(BzAsp)_n$.

It was assumed that there was a random distribution of parallel ("up") and the antiparallel ("down") helices in the ω structure of the polymer similar to the situation shown to exist for poly(L-alanine) by Elliott and Malcolm[10] and this led to good but not excellent agreement between the observed X-ray diffraction intensities and those calculated from the model. The situation was complicated because some of the equatorial diffraction intensities varied from sample to sample. The closest approach distances between the atoms on this model were comparable with typical van der Waals distances for adjacent up or adjacent down helices, but there were some short contacts of up helices adjacent to down helices.

Recently McGuire *et al.*[11] have calculated minimum energy conformations for the ω helix in $(BzAsp)_n$ in essential agreement with most of the infrared data. However, the benzene ring orientations would seem to disagree with the infrared data and to favor intermolecular interactions.

Happey *et al.*[12] have carried out proton magnetic resonance (pmr) studies on the ω form of $(BzAsp)_n$ and suggest that reorientational motion of the benzene rings occurs at temperatures well above −100°, and that the ω structure has benzene ring positions C which are intermediate between the positions A and B proposed by Bradbury *et al.* at low temperatures. However, the position C which these authors propose would not take advantage of the energy gained if the benzene rings are touching as in the positions A and B, so that maximum advantage is taken of van der Waal's interactions in the stacked benzene rings.

In this present work a study of the structures of the ω form of $(BzAsp)_n$ has been attempted using electron diffraction, which has proved a very suitable technique for studies of polypeptide structures.[13] This work together with characterization studies using infrared absorption and the earlier X-ray results[5] has been used to show that a well-defined ω structure exists and a model for the packing of the ω helices is proposed which gives rather better agreement with the diffraction results than a model

(1) R. H. Karlson and E. R. Blout, *J. Amer. Chem. Soc.*, **80**, 1259 (1958).
(2) E. M. Bradbury, A. R. Downie, A. Elliott, and W. E. Hanby, *Proc. Roy. Soc., Ser. A*, **259**, 110 (1960).
(3) B. R. Malcolm, *Nature (London)*, **219**, 929 (1968).
(4) B. R. Malcolm, *Biopolymers*, **9**, 911 (1970).
(5) E. M. Bradbury, L. Brown, A. R. Downie, A. Elliott, R. D. B. Fraser, and W. E. Hanby, *J. Mol. Biol.*, **5**, 230 (1962).
(6) L. Bragg, J. C. Kendrew, and M. F. Perutz, *Proc. Roy. Soc., Ser. A*, **203**, 321 (1950).
(7) I. F. McLuckie, M.S. Thesis, London, 1969.
(8) R. M. Stephens, Ph.D. Thesis, London, 1968.
(9) E. M. Bradbury, B. G. Carpenter, and R. M. Stephens, *Biopolymers*, **6**, 905 (1968).
(10) A. Elliott and B. R. Malcolm, *Proc. Roy, Soc., Ser. A*, **249**, 30 (1959).
(11) R. E. McGuire, G. Vanderkooi, F. A. Momany, R. T. Ingwall, G. M. Crippen, N. Lotan, R. W. Tuttle, K. L. Kashuba, and H. A. Scheraga, *Macromolecules*, **4**, 112 (1971).
(12) F. Happey, D. W. Jones, and B. M. Watson, *Biopolymers*, **10**, 2039 (1971).
(13) B. K. Vainshtein and L. I. Tatarinova in "Conformation of Biopolymers," G. N. Ramachandran, Ed., Pergammon Press, New York, N. Y., 1967, pp 569–581.

with a random distribution of parallel and antiparallel helices.

Experimental Section

Preparation of Samples. The $(BzAsp)_n$ used for all these studies was a single sample obtained from Pilot Chemicals; the molecular weight was given as 245,000 and its ability to provide films with a high degree of orientation indicated that it was of high molecular weight.

Oriented films for electron diffraction and infrared absorption studies were produced in several ways. For the left-handed helical conformation some films were obtained by unidirectional shearing to dryness of a concentrated chloroform solution on a glass plate with a groundhorn spatula; the film was floated off the plate on water. An improvement on this technique was found by allowing a drop of solution (12 mg ml^{-1}) to evaporate on a clean, distilled-water surface. The multilayer film was picked up on grids for electron diffraction studies and on barium fluoride plates for infrared spectroscopy. The degree of orientation in the samples is critically dependent on the concentration of the polypeptide solution and is presumably due to viscous flow of the polypeptide in the chloroform solution as the chloroform is evaporating on the water surface. A useful modification of the above technique is to place a drop of the solution (12 mg ml^{-1}) onto a glass slide and to cover it immediately with a second glass slide to prevent evaporation of the chloroform. The slides are sheared apart and one of them is immediately dipped into a distilled-water trough at about 30° to the surface. The polypeptide solution elongates by a factor of about two as it shoots onto the water surface with the chloroform evaporating.

Right-handed helical samples were produced by the monolayer technique developed by Malcolm.[3,4] A monolayer of the polypeptide was formed from a drop of solution in chloroform (placed on the surface of distilled water in a Langmuir trough). The monolayer was then compressed for 1 or 2 min to give a collapsed film.

The ω-helical form of $(BzAsp)_n$ was obtained by heating films of either helix sense under vacuum to 140°.

Infrared Spectroscopy. Infrared spectra were recorded on a Grubb-Parsons spectrometer, the Spectromaster, over the range 4000 to 800 cm^{-1}. Frequency–conformation correlations previously described[9] were used to characterize the helix sense and conformations of the unheated and heated $(BzAsp)_n$ films.

Electron Diffraction. Electron diffraction studies were made using a Phillips E.M. 300 electron microscope. As polymer films and particularly polypeptide films are very prone to electron-beam damage,[14] electron diffraction patterns were taken with a low flux of 100-kV electrons over a selected area of specimen of diameter 40 μ.

Results

Infrared Absorption Measurements. Films cast from chloroform either on plates or as multilayers on a water surface were found to give amide band frequencies of 1667 cm^{-1} for the amide I, 1558 cm^{-1} for the amide II, and dichroisms of side-chain vibrations all characteristic of the left-handed helical form. Films of the collapsed monolayers gave spectra with an amide I at 1658 cm^{-1} and an amide II at 1552 cm^{-1} and side-chain band dichroisms all characteristic of the right-handed helical conformation.[9] This agrees with the work of Malcolm.[3]

On heating films of left-handed α-helical $(BzAsp)_n$ to 140° under vacuum, a polymorphic transition takes place to another helical form, the ω helix thought also to be a left-handed helix.[5] This transition was observed for all the left-handed helical forms of $(BzAsp)_n$ and the infrared spectra obtained were identical with those already described for the ω helix.[5] Whether the right-handed α-helical form of $(BzAsp)_n$ is able to undergo a similar polymorphic transition is of some interest and Malcolm[4] has found that such a change takes place on heating films of the collapsed monolayer. The resulting infrared spectrum however was the same as that for the ω helix obtained from the left-handed form of $(BzAsp)_n$. These results have been confirmed in this study and if the similarity of the spectra is taken to indicate the same helix sense and side-chain conformation then, as pointed out by Malcolm,[4] considerable molecular rearrangement must occur in the solid film of the right-handed $(BzAsp)_n$ on heating to result in a transition both of helix sense and type.

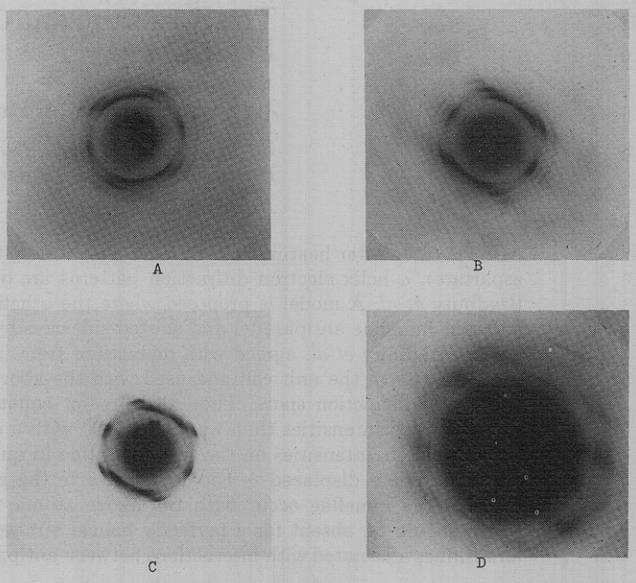

Plate 1. Electron diffraction patterns from ω $(BzAsp)_n$. (A) Sample prepared by the monolayer technique; (B) sample prepared by viscous flow technique from chloroform solution; (C) sample prepared by stroking from chloroform solution (light exposure); (D) sample prepared by stroking from chloroform solution (heavy exposure).

Diffraction Studies of the ω Form of Poly(β-benzyl L-aspartate). Electron diffraction patterns from the right- and left-handed helical unheated forms of the polypeptide have few diffraction spots. In both cases however clear meridional reflections occur in the region of 1.5 Å, indicating that both the left- and right-handed forms of the unheated polypeptide contain α-like helices.

Electron diffraction patterns of the heated polypeptide prepared by compressing monolayers and by the viscous flow technique are shown in Plate 1A,B. Plate 1C,D shows two diffraction patterns of the ω structure from samples prepared by stroking out films. All these diffraction patterns are similar in the d spacings, and in the relative intensities of diffraction spots. The d spacings are identical with those obtained from X-ray data.[5] All the diffraction spots in Plate 1 can be indexed and their d spacings give values for the tetragonal unit cell dimensions of $a = b =$ 13.88 Å and $c = 5.3$ Å. These lattice parameters yield a density of 1.337 cm ml^{-1} in agreement with measured values.[5]

ω helices with a $P4_3$ space group should yield a meridional reflection on the fourth-layer line of the electron diffraction pattern and other meridional reflections are not allowed theoretically because of the rules for selecting the order of the Bessel functions in the Fourier transform of the helices. However, Plate 1A–D illustrates that reflections at 001, 002, and 003 occur as well as at 004 and this is true of all electron diffraction patterns from the ω structure, indicating distortions from a true helical structure. In Plate 1A–D the {110} and {330} equatorial reflections are missing and this is true of all our diffraction patterns from the heated polymer however the specimens were prepared.

In order to estimate the electron diffraction intensities against the background due to inelastically scattered elec-

(14) K. Kobayashi and K. Sakaoku, *Lab. Inv.*, 14, 359 (1965).

trons, densitometer traces were taken from the diffraction photographs and the procedure outlined by Vainshtein[15] was followed. The equatorial diffraction intensities for some ten ω-helix diffraction patterns were averaged to provide reliable estimates of the normalized intensities. There were a few samples which gave ω-helix diffraction patterns with slightly different diffraction intensities from the majority of samples as was the case with the X-ray studies.[5] This could be because of some preferred orientation of the crystallites of the polymer about the fiber-axis direction. The diffraction intensity measurements from these samples were excluded from the estimates of intensities described above because these samples were not typical.

Figure 1A shows the observed intensities of the equatorial electron diffraction spots normalized to the intensity of the 300 reflection, plotted against the inverse of d spacing. The intensities in the figure are corrected values and the corrections applied are those outlined by Vainshtein,[15] which correspond to the corrections derived from Arnott[16] in the limit of small wavelength. These corrections are based on the fact that diffraction spots are (relatively) weighted in a way determined by the angular distribution of the small fiber crystallites (*i.e.*, texture patterns) each of which have finite-sized interference regions in reciprocal space yielding a diffraction when they intersect the reflection sphere. Assuming (for the present), that all planes of the type $\{hkl\}$ contribute equal diffraction intensities, that there is a random distribution of crystallite orientations about the fiber-axis direction and that there is arcing due to a distribution of fiber-axis directions, then the intensity measured by a microdensitomer at a spot at the center of a diffraction arc should be

$$I \propto |F|^2 P d_{hkl} d_{hk0}$$

where F is the structure factor and P is the multiplicity of the $\{hkl\}$ reflections. All observed intensities therefore were corrected by dividing by the appropriate multiplicities and in the case of equatorial reflections dividing by $d_{hkl}d_{hk0}$ or d^2_{hk0}. It is these corrections which are involved in the intensities plotted in Figure 1A.

In Figure 1B the corrected observed X-ray intensities of Bradbury *et al.*[5] are plotted against $1/d$. Figure 1A,B shows how similar the X-ray and electron diffraction intensities are in spite of the fact that the relative scattering amplitudes for the atoms O, C, N, and H are different for electron and X-ray diffraction. However, O, C, and N have similar atomic numbers so one would expect an approximate agreement between the X-ray results and the electron diffraction results if the ω form of $(BzAsp)_n$ is a well-defined structure and independent of the wide variety of specimen preparation techniques used in the electron and the X-ray diffraction studies.

Analysis of Results

Comparison with a Model of Random up and down Helices. Taking the atomic coordinates for the ω structure given by Bradbury *et al.*[5] with their model of a random distribution of up and down helices, the intensities for diffraction spots were calculated using a structure factor calculation computer program for their position A for the benzene ring. These intensities are plotted in Figure 1D for X-rays. The program was modified to perform the same calculation using electron atomic scattering amplitudes and the predicted electron diffraction intensities are shown plotted against $1/d$ in Figure 1C. R_2 values quoted in Figure 1 were calculated from the data of Figure 1C,D. These values are the sum of the differences between observed and calculated diffraction intensities divided by the sum of the observed intensities. The calculated intensities are normalized so that the sum of the intensities are the sum of the observed intensities for these calculations. For small R_2 values the usually quoted R values for diffraction amplitudes are approximately $\frac{1}{2}R_2$.[15]

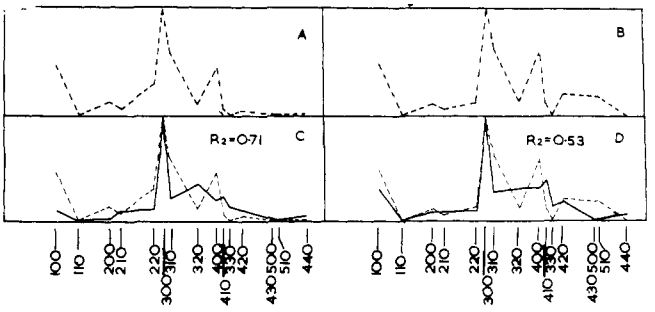

Figure 1. (A) Electron diffraction observed intensities (corrected); (B) X-ray diffraction observed intensities (after Bradbury *et al.*); (C) calculated intensities for electron diffraction using coordinates of Bradbury *et al.* with random distribution of up and down helices (R_2 = 0.71); (D) calculated intensities for X-ray diffraction; conditions as in part C (R_2 = 0.53). (- - - - - - - - - -) Corrected observed intensities.

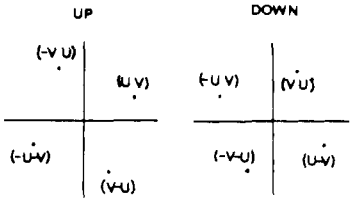

Figure 2. $(BzAsp)_n$ equivalent positions for up and down helices in C-axis projection.

The model does not predict zero intensity for the 330 reflection nor does it predict a peak at the 400 diffraction spot as well as other differences. In view of the agreement of the model of Bradbury *et al.*[5] with the infrared data, one would expect a rather better agreement between the predicted and observed diffraction intensities.

Calculations for the position B of the benzene rings are essentially the same as for the A position as far as equatorial reflections are concerned. Calculations of diffraction intensity for the position C suggested by Happey *et al.*[12] did not show very good agreement with the electron diffraction equatorial intensities.

The fact that the (110) and (330) reflections are absent in both X-ray *and* electron diffraction in spite of the different relative atomic scattering factors possibly indicates systematic absences which could be due to a particular type of molecular packing.

A Model for the Packing of ω Helices in the Heated Polypeptide. It is instructive to consider what packing geometries for parallel (up) and antiparallel (down) ω helices in a tetragonal lattice will account for absent equatorial reflections in a diffraction pattern. If we take the scattering from selected atoms in equivalent positions in an up helix, with the helix at the origin of the unit cell as shown in Figure 2, then the contribution to the scattering amplitude for an $hk0$ reflection from these atoms is given by

$$F_{up} = f_{at}\{e^{2\pi i(hu+kv)} + e^{2\pi i(-hv+ku)} + e^{2\pi i(-hu-kv)} + e^{2\pi i(hv-ku)}\}$$

(15) B. K. Vainshtein, "Structure Analysis by Electron Diffraction," Pergammon Press, New York, N. Y., 1964.
(16) S. Arnott, *Polymer*, 6, 478 (1965).

where f_{uv} is the scattering amplitude for the atoms at the chosen equivalent positions. The contribution for a down helix would be

$$F_D = f_{uv}\{e^{2\pi i(hv+ku)} + e^{2\pi i(-hu+kv)} + e^{2\pi i(-hv-ku)} + e^{2\pi i(hu-kv)}\}$$

If the unit cell were to contain two helices, an up helix at (0,0,0) and a down helix at ($\frac{1}{2}$,$\frac{1}{2}$,w) there would be absent reflections as noted for the ω form of poly[β-(*p*-chlorobenzyl L-aspartate] by Takeda *et al.*,[17] where the ω helices are packed in a tetragonal lattice with a = 23.3 Å and c = 5.20 Å.

As pointed out by Bradbury *et al.*[5] one might choose a larger unit cell than they chose for poly(β-benzyl L-aspartate) which could accommodate an up and a down helix. However, this would lead to extra diffraction spots even though the {100}, {300}, and {500} reflections might be systematically absent. These extra diffraction spots are not observed and so we must conclude that the X-ray unit cell dimensions are essentially correct.

In the work of Takeda *et al.*[17] a random distribution of up and down α helices of their unheated polypeptide agreed with the diffraction analysis whereas on heating the polypeptide a systematic distribution of up and down helices occurred. This suggests that on heating the polypeptide there was either a large amount of molecular movement or intramolecular atomic movement.

One must question whether, in any helical polymer sample it is realistic that there should be completely random arrangement of up and down helices. Such an arrangement must usually be a metastable situation which is frozen in during the final stages of fiber orientation from a solvent due to a lack of molecular mobility, so that the true minimum energy situation cannot occur. Alternatively if there are long repeat distances along the helical axis coupled with a polydispersity of molecular weight, intermolecular interactions would not be sufficiently regular for there to be a large energy difference between interactions with parallel helices and interactions with antiparallel helices.

In any situation with a reasonable degree of molecular mobility and regular interactions such as occurs in the ω structure, there must be either blocks of up helices and blocks of down helices packed together or blocks with molecules packed antiparallel such as reported by Takeda *et al.*[17] It would be a coincidence if the interaction energy for the antiparallel molecular packing were the same as for the parallel packing so that one situation must usually have the lower energy, making blocks of one type of molecular packing more favorable. Of course, the blocks of packed helices must be distributed to produce equal numbers of up and down helices over a whole specimen, since the techniques of fiber orientation do not usually discriminate in favor of either direction.

The model we have in mind for the packing of ω helices in $(BzAsp)_n$ is where the lowest energy situation is for molecules to be packed parallel in lamellae. There will be some lamellae with up helices packed together and some with packed down helices within one crystallite. This situation is illustrated in Figure 3 and lamellae with down helices are displaced by half-lattice spacing in the x-axis direction relative to those with up helices. With this model the size of the unit cell is determined by the packing within the lamellae providing that the numbers of molecules in the thicknesses of the lamellae are not constant and provided the lamellae are more than one molecule thick.

(17) Y. Takeda, Y. Iitaka, and M. Tsuboi, *J. Mol. Biol.*, 51, 101 (1970).

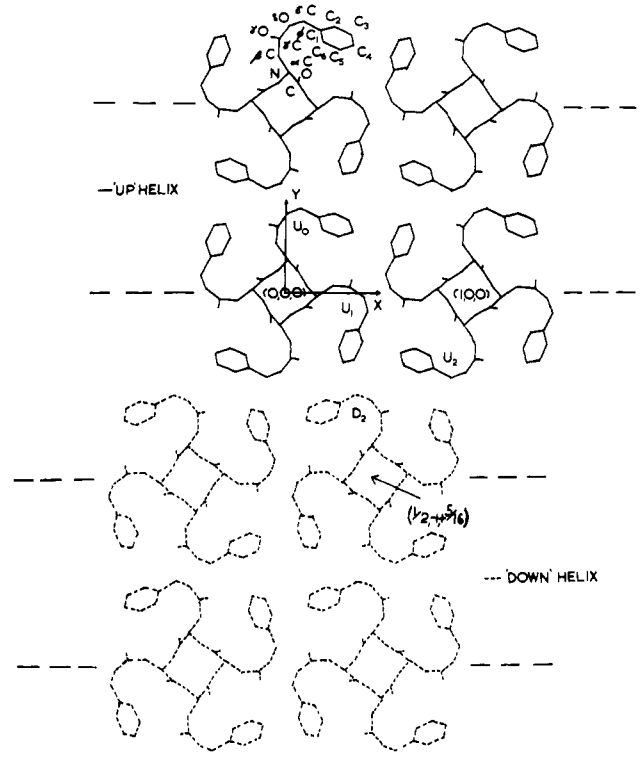

Figure 3. *C*-axis projection of ω helices in poly(β-benzyl L-aspartate) illustrating the model of up and down lamella. The coordinates are those of Bradbury *et al.* (1962), rotated 5° anticlockwise in the unit cell.

Neglecting for the present problems associated with molecular averaging and interference regions in reciprocal space due to misoriented finite-sized crystallites with such a lamella structure, we propose that the scattering amplitude will be approximated by adding the contribution due to an up helix at the origin of the unit cell with that due to a down helix at ($\frac{1}{2}$,0,w). Thus the contribution to the amplitude due to the equivalent positions of the type uv is

$$\begin{aligned}\Delta F_{hk0} &= \Delta F_{up} + \Delta F_D e^{\pi ih} \\ &= \Delta F_{up} - \Delta F_D \text{ (for } h \text{ odd)} \\ &= \Delta F_{up} + \Delta F_D \text{ (for } h \text{ even)}\end{aligned}$$

The value of ΔF_{hk0} for these circumstances is zero when $h = k$ = odd and when h = odd with $k = 0$. The h = odd, $k = 0$ absences would not be noticed in a diffraction pattern with a random distribution of crystallite orientations in the plane perpendicular to the fiber axis direction, since diffraction from $h = 0$, k = odd reflections of the same d spacing in the tetragonal structure would produce diffraction spots in the same positions. However, the $h = k$ = odd absences would be observed and this possibly explains the absence of the 110 and 330 reflections in the ω-helix electron and X-ray diffraction patterns.

Following the argument a stage further one might expect half-lattice spacing shifts between blocks of up helices and blocks of down helices in directions x and y. In this case one would have up helical blocks at (0,0,0) and ($\frac{1}{2}$,$\frac{1}{2}$,0) and down helical blocks at (0,$\frac{1}{2}$,w) and ($\frac{1}{2}$,0,w). This would lead to more systematic absences which are not observed in practice. However, blocks of up helices and down helices displaced at the equivalent unit cell positions above would have to leave vacant molecular sites at the corners of the blocks; this is energetically unfavorable and further it would lead to a difference between measured densities and those calculated using unit cell

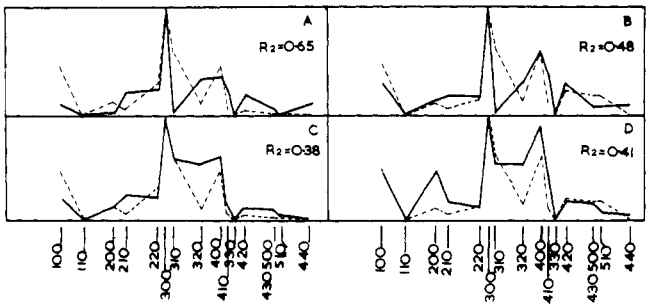

Figure 4. (A) Calculated electron diffraction intensities using the lamella model with down helices displaced $a/2$ in the x direction (coordinates of Bradbury *et al.*) (R_2 = 0.65); (B) calculated X-ray diffraction intensities with conditions as in part A (R_2 = 0.48); (C) calculated electron diffraction intensities using the lamella model with down helices displaced $a/2$ in the x direction (coordinates rotated 5° from those given by Bradbury *et al.*) (R_2 = 0.38); (D) calculated X-ray diffraction intensities with conditions as in part C (R_2 = 0.41). (--------) Corrected observed intensities.

dimensions. As already mentioned these two densities in fact agree.

The model of lamellae of up and down helices seems the more favorable situation energetically.

Assessment of Diffraction Intensities Using the Lamella Model. Taking the atomic corrdinates for the ω structure in poly(β-benzyl L-aspartate) proposed by Bradbury *et al.*[5] for a left-handed helix, the diffraction intensities can be calculated using the model where the down helices are displaced by half-lattice spacing in the x-axis direction of the tetragonal unit cell while the up helices are at the unit cell origin. The calculation leads to different amplitudes for different planes of an $\{hkl\}$ family since the scattering amplitude relations for a space group $P4_3$ are

$$|F(hkl)| = |F(\bar{h}\bar{k}\bar{l})| = |F(hk\bar{l})| \neq |F(\bar{h}kl)|, \quad |F(\bar{h}kl)| = |F(h\bar{k}l)|$$

In order to make comparisons with the experimental data of Figure 1A,B, the intensities for all planes of an $\{hkl\}$ type were summed in the calculations from the lamella model and the sum was divided by the total number of planes. Thus the effective mean intensity for each diffraction spot was calculated.

The graphs of the above-calculated mean intensities plotted against the inverse of d spacing are given for electron diffraction in Figure 4A and for X-ray diffraction in Figure 4B and again R_2 values are given. From these two figures there is reasonable agreement between the theoretically predicted curves and the experimentally observed diffraction intensities. There are intensity maxima at the 300 and 400 diffraction spots and the 330 and 110 reflections are absent in both cases. However, there is a discrepancy in that the 310 diffraction intensity is much too low for the calculations from the lamella model compared with the observed intensity.

To see what corrections should be applied to the model a projection of the structure onto the basal plane was obtained from the X-ray diffraction results of Bradbury *et al.*[5] in the following way. The signs of the diffraction amplitudes for a given $(hk0)$ plane were chosen to be the same as those calculated from the lamella model structure amplitudes described above. However it was not possible to ascribe amplitudes immediately for each plane from the observed diffraction pattern because the observed diffraction spots are a multiplicity from all $\{hk0\}$ planes, and planes of the type (hkl) scatter differently from those of the type $(\bar{h}kl)$ for the $P4_3$ structure. Therefore diffraction

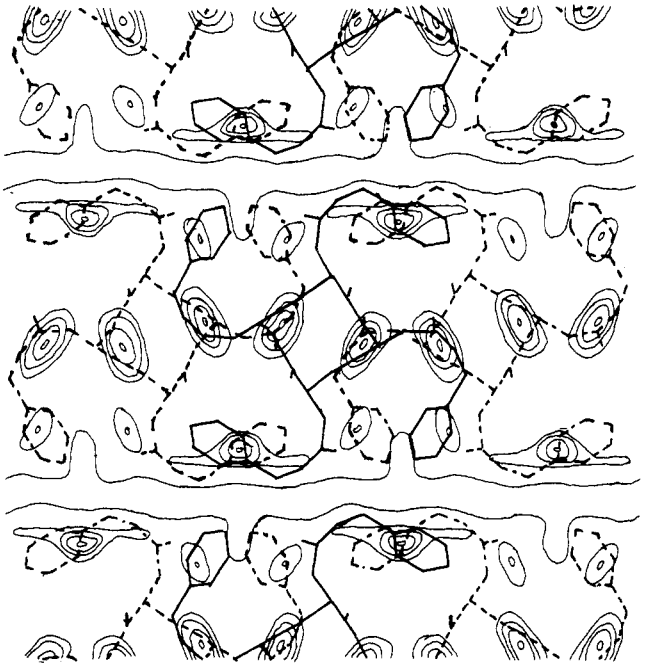

Figure 5. Fourier synthesis from the observed X-ray equatorial reflections. Synthesis assumes the signs of diffraction amplitudes calculated from the lamella model. (——) Up helix with coordinates given by Bradbury *et al.*; (-----) down helix with coordinates given by Bradbury *et al.*

amplitudes were ascribed to the various (hkl) planes by apportioning the observed intensities among these planes in the same ratios as was calculated from the model described above. This data was put into a Fourier synthesis program and a projection of the structure onto the basal plane obtained. This is shown in Figure 5.

Figure 5 needs some explanation since clearly the projection does not have the fourfold symmetry expected from the $P4_3$ structure. We should stress here again that the model used to calculate the signs of the amplitudes used to calculate Figure 5 was a model of lamellae of packed up helices displaced half a lattice spacing from lamellae of packed down helices. Taking into account the statistical adding of vectors for the variable thickness lamellae we believe that effectively one has to work out scattering from an up helix at (000) and a down helix at $(\frac{1}{2}0w)$, in the same way as one superimposed up and down helices for calculations involving a random distribution of up and down helices. Clearly in our case in the calculation of diffraction amplitudes, the fourfold symmetry is lost, and this of course occurs in the synthesis as well since the signs of diffraction amplitudes were chosen from the structure factor calculations.

In Figure 5 we sketched in the projection of up and down helices; the former at the origins of the unit cells and the latter at $(\frac{1}{2}0w)$ coordinates. These are the projections of the atoms using the coordinates given by Bradbury *et al.*[5] and again we should remember that Figure 5 represents a statistical result and really the helices are packed parallel, one per unit cell, in lamellae.

It is clear that the projection agrees very well with the model using the above atomic positions. In particular one can see clear troughs around which the residues bend. One can also see clear maxima near to the benzene rings and where the up helices and the down helices overlap in the unit cell. The structure on close inspection is fairly convincing. However, it is noticeable that the benzene rings drawn from the model of Bradbury *et al.* overlap into the trough regions in the synthesis. A rotation of the

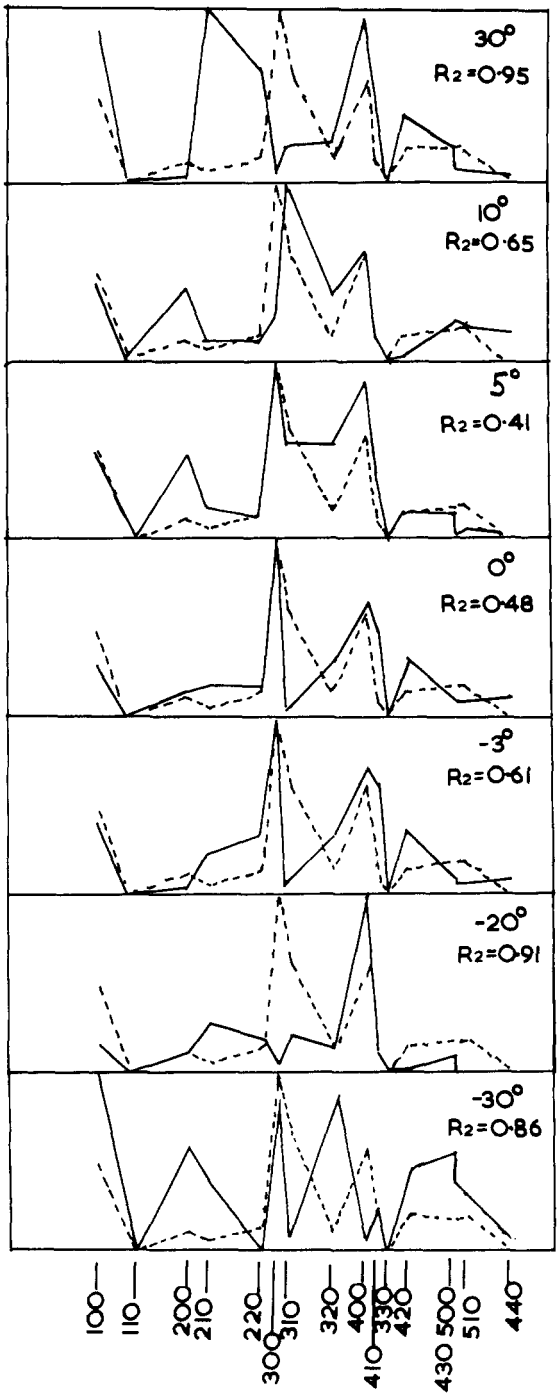

Figure 6. Calculated X-ray diffraction intensities for various rotations of the coordinates given by Bradbury *et al.* (1962), assuming the lamella model with down helices displaced $a/2$ in the x direction.

helices through 5° anticlockwise improves the fit considerably.

In view of this the atomic coordinates were refined using trial and error methods as follows. Taking the atomic coordinates of Bradbury *et al.*,[5] the helices were rotated in the unit cell at several angular intervals over the whole 90° rotation which would bring the projection back into position. The equatorial diffraction intensities using the lamella model are plotted in Figure 6 for several angular positions of the helices and R_2 values for diffraction intensities are quoted. Several positions are shown in the figure around the angles where the R_2 values are low. It can be seen that as the helix rotation approaches 5° anticlockwise

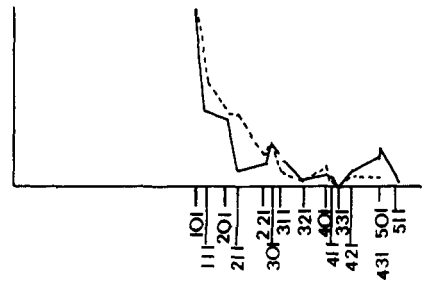

Figure 7. (A, - - - - -) Corrected observed first-layer line intensities normalized to the 101 intensity; (B, ——) calculated intensities assuming the lamella model with down helix lamellae displaced $5c/16$.

the predicted diffraction intensities approach those observed. The R_2 value reaches a minimum of 0.4 corresponding to an R_1 value of about 0.2. At any appreciable angle from the 5° position the calculated intensities become badly related to the observed intensities with high R_2 values.

On rotating 5° anticlockwise the intensity of the (310) reflection has increased considerably to about the experimentally observed value. The theoretically calculated diffraction intensities on the lamella model agree in most details with the experimental intensities for both X-ray and electron diffraction. This is shown for comparison with previous calculations in Figure 4C for electron diffraction and Figure 4D for X-ray diffraction. However, the calculated intensity of the (320) reflection is high. Bearing in mind the errors of estimation of diffraction intensities for X-ray and electron diffraction, the agreement between these 5° rotated intensities (Figure 4C,D) and the observed intensities (Figure 1A,B) is reasonable. If we estimate R_2 values from the observed and calculated equatorial diffraction intensities we obtain a value 0.38 for electron diffraction and 0.41 for the X-ray results which correspond to R_1 values in the neighborhood of 0.2.

Diffraction intensities were calculated to see what movements of the side chain would tend to change the 5° rotated helix intensity calculations in a direction to bring them into better agreement with the observed intensities. By rotating about all the bonds in the side chain it was found that small rotations clockwise and anticlockwise tended to correct certain reflections in the direction toward agreement with the observed intensities, but other reflection intensities moved away from the observed values. It was therefore not possible to rotate about any of the bonds to improve the 5° rotated diffraction pattern. This is quite satisfactory since rotation about the bonds in the side chains changes the conditions which were already in good agreement with the infrared data.[5,8,9]

The intensities of the diffraction spots on the first-layer line were measured from the electron diffraction plates. These intensities relative to the 101 reflection are corrected for multiplicity and for the distribution of crystallite orientations as described earlier. Figure 7A shows these corrected intensities plotted against the inverse of d spacing. It is very clear that the 101 diffraction spot is very intense relative to the other diffraction spots.

Taking the lamella model with helices rotated 5° anticlockwise compared with the coordinates of Bradbury *et al.*[5] the expected first-layer line diffraction intensities have been calculated for various z displacements between the two types of helix in intervals of $c/16$. Amplitudes for the structure with the A position and with the B position of the benzene rings have been added since it is likely that both positions will be equally occupied at room tem-

Table I
Coordinates of Residue O of an Up Helix in Ångströms[a]

x_0	y_0	z_0	Atom
0.34	2.52	0	αC
1.051	1.64	1.05	C′
1.10	2.00	2.25	O
−0.56	1.71	−0.80	N
−0.49	3.63	0.70	Cβ
−0.43	4.95	−0.13	C′γ
−1.09	5.03	−1.14	Oγ
0.35	5.93	0.30	Oδ
1.36	6.38	−0.68	εC
2.71	5.68	−0.45	ϕC_1
3.76	5.95	−1.30	ϕC_2A
5.02	5.33	−1.13	ϕC_3A
5.21	4.45	−0.08	ϕC_4
4.15	4.15	0.83	ϕC_5A
2.34	4.75	0.70	ϕC_6A
3.56	6.06	0.70	ϕC_2B
4.79	5.46	0.83	ϕC_3B
4.40	4.06	−1.13	ϕC_5B
3.12	4.66	−1.30	ϕC_6B

[a] These are the same as those given by Bradbury *et al.*[5] rotated anticlockwise. A and B refer to the two benzene ring positions proposed by these authors. Atoms in other residues of the up helix are at $x_1 = y$, $y_1 = -x_0$, $z_1 = z_0 + 1.325$ Å; $x_2 = -x_0$, $y_2 = -y_0$, $z_2 = z_0 + 2.65$ Å; $x_3 = -y_0$, $y_3 = x_0$, $z_3 = z_0 + 3.975$ Å. On the model discussed, atoms in residue O of a down helix are at $\bar{x}_0 = x_0 + 6.94$ Å, $\bar{y}_0 = -y_0$, $\bar{z}_0 = -z_0 + 1.66$ Å.

perature and rotations between the two stable states may occur as indicated by the pmr results of Happey *et al.*[12] There is good agreement with the observed intensity ratios normalized to the (101) reflection for displacements $-c/4$ and $+5c/16$ of the down helix lamellae where we have adopted the coordinate conventions of Bradbury *et al.*[5] which are also given in Table I. Both displacements give a number of interatomic distances between lamellae which would yield favorable van der Waal's interactions. The most favorable situation it would seem is a displacement of $+5c/16$ (1.66 Å) for the down helix lamellae, since for this case there is better agreement between the theoretical and experimental ratios between the (101) and (300) diffraction intensities (1.4 theoretically and 1.3 experimentally).

Figure 7B shows the predicted first-layer line intensities for the displacement $+5c/16$ between lamellae along the fiber-axis direction. The agreement with Figure 7A is good except for the 211 reflection where the calculations predict too low an intensity.

Table I shows the atom coordinates in the unit cell which statistically contains up helices centered at (0,0,0) and down helices at $(\frac{1}{2},0,+\frac{5}{16})$, following the coordinate conventions used by Bradbury *et al.*[5]

Table II shows contact distances between parallel helices and between up helices and down helices on the lamella model. In the table intermolecular atomic distances are given when they are less than 4 Å. If we compare these distances with those of Bradbury *et al.*[5] which referred to a random distribution of up and down helices, we find the contacts between parallel helices are similar in the two cases, but for the 5° rotated coordinates there are contacts between the residues in the neighborhood of the δ oxygens. In the case of the $a/2$ displaced helices in lamellae there are many contacts to provide good van der Waals interactions between lamellae. However, there is one very short contact between carbon atoms, but there is good evidence from the presence of the extra meridional diffraction arcs that the residues between antiparallel helices are distorted from atomic positions which would form perfect ω helices.

Table II
Interatomic Distances between Helices[a]

Code of Atoms and Distance between	Separation (Å)	Approx van der Waals Separations (Å)[b]
Distances between Parallel Helices		
(0,0,0),$U_0\beta C$ and (0,0,0),U_0O	2.75	3.1
(0,0,0),$U_0,\beta C$ and (0,0,−1),U_3,O	2.95	3.1
(0,0,0),$U_0,\phi C_4$ and (1,0,−1),$U_3,\phi C_1$	3.83	3.4
(0,0,0),$U_0,\phi C_4$ and (1,0,0),$U_3,\phi C_2A$	3.91	3.4
(0,0,0),$U_0,\phi C_4$ and (1,0,−1),$U_3,\phi C_2A$	3.77	3.4
(0,0,0),$U_0,\phi C_4$ and (1,0,−1),$U_3,\phi C_2B$	2.78	3.4
(0,0,0),$U_0,\phi C_4$ and (1,0,−1),$U_3,\phi C_3B$	3.23	3.4
(0,0,0),$U_0,\phi C_4A$ and (1,0,0),$U_3,\phi C_2A$	3.69	3.4
(0,0,0),$U_0,\phi C_3A$ and (1,0,−1),$U_3,\phi C_2A$	3.60	3.4
(0,0,0),$U_0,\phi C_3A$ and (1,0,−1),$U_3,\phi C_2B$	3.30	3.4
(0,0,0),$U_0,\phi C_3B$ and (1,0−1),$U_3,\phi C_2B$	3.83	3.4
(0,0,0),$U_0,\phi C_3A$ and (1,0,−1),$U_3,\phi C_3A$	3.75	3.4
(0,0,0),$U_0,\phi C_3A$ and (1,0,−1),$U_3,\phi C_3B$	3.47	3.4
(0,0,0),$U_0,\phi C_3B$ and (1,0,−1),$U_3,\phi C_3B$	3.90	3.4
(0,0,0),$U_1,\delta O$ and (1,0,0),$U_3,\delta O$ also (1,0,−1),$U_3\delta O$	3.39	2.8
(0,0,0),$U_1,\delta O$ and (1,0,0),$U_3,\epsilon C$	2.84	3.1
(0,0,0),$U_1,\gamma C$ and (1,0,0),$U_3,\epsilon C$	3.41	3.4
(0,0,0),$U_1,\gamma O$ and (1,0,0),$U_3,\epsilon C$	3.28	3.1
Distances between Antiparallel Helices (between Lamellae)		
(0,0,0,$U_1,\phi C_4$ and $(\frac{1}{2},-1,\frac{5}{16}),D_2,\phi C_1$	3.47	3.4
(0,0,0),$U_1,\phi C_4$ and $(\frac{1}{2},-1,\frac{5}{16}),D_2,\epsilon C$	2.96	3.4
(0,0,0),$U_1,\phi C_4$ and $(\frac{1}{2},-1,\frac{5}{16}),D_2,\phi C_2A$	3.12	3.4
(0,0,0),$U_1,\phi C_3A$ and $(\frac{1}{2},-1,\frac{5}{16}),D_2\delta O$	3.48	3.1
(0,0,0),$U_1,\phi C_3A$ and $(\frac{1}{2},-1,\frac{5}{16}),D_2\epsilon C$	2.55	3.4
(1,0,0),$U_2,\phi C_3A$ and $(\frac{1}{2},-1,\frac{5}{16}),D_2\gamma O$	3.84	3.1
(1,0,0),$U_2,\phi C_2A$ and $(\frac{1}{2},-1,\frac{5}{16}),D_2\gamma O$	3.74	3.1
(0,0,−1),$U_1,\phi C_4$ and $(\frac{1}{2},-1,\frac{5}{16}),D_2,\phi C_2B$	3.66	3.4
(0,0,−1),$U_1,\phi C_3B$ and $(\frac{1}{2},-1,\frac{5}{16}),D_2,\delta O$	3.80	3.1
(0,0,0),$U_1,\phi C_3B$ and $(\frac{1}{2},-1,\frac{5}{16}),D_2,\epsilon C$	3.64	3.4
(0,0,−1),$U_1,\phi C_3B$ and $(\frac{1}{2},-1,\frac{5}{16}),D_2,\epsilon C$	3.90	3.4
(1,0,−1),$U_2,\phi C_3B$ and $(\frac{1}{2},-1,\frac{5}{16}),D_2,\gamma C$	3.95	3.4

[a] The coordinates of the origins of the helices are given in parentheses and match those of Figure 3. A and B refer to the two benzene ring positions. [b] Neglecting H atoms.

Discussions and Conclusions

Electron diffraction studies of the ω form of poly(β-benzyl L-aspartate) have added information to the earlier X-ray studies of Bradbury *et al.*[5] In the first place the absence of 110 and 330 reflections in both studies suggests that there may be systematic absences associated with the packing of the ω helices rather than chance zero intensity reflections; secondly, the electron diffraction intensity measurements have added information to the X-ray intensities and hence can be combined with the X-ray results in a search for the structure; thirdly, the consistency of the results by electron diffraction on heating both from the left-handed α-helical form of the polypeptide and from the right-handed form, coupled with infrared measurements, suggests that there is a unique ω-helix structure which could be solved; fourthly, the electron diffraction patterns from polypeptides give more diffraction spots than X-ray diffraction in a single diffraction pattern because the electron reflection sphere is nearly a plane section through the reciprocal lattice on account of the

smaller wavelength, and it therefore intersects meridional reciprocal lattice points. This last advantage shows up meridional reflections on the first-, second-, and third-layer lines in Plate 1A–D which should not be allowed according to diffraction theory from perfect ω helices since the Fourier transform of the unit cell should be zero at these points. There must therefore be distortions in the ω helices.

A lamella model for the packing of ω helices in poly(β-benzyl L-aspartate) suggested herein fits the X-ray and electron diffraction intensities quite well (with an R_1 factor of about 0.2). In analyzing this model it was assumed that molecular averaging would lead to a Fourier transform equivalent to antiparallel helices at unit-cell-zero coordinates (0,0,0) and ($\frac{1}{2}$,0,+$\frac{5}{16}$) which would mean absent (110) and (330) reflections. This assumption can be shown to be reasonable by the following argument.

Diffraction from one single thin lamella of packed up helices will yield interference regions in reciprocal space at the reciprocal lattice points corresponding to the parallel packing of helices within the lamella. The interference region for each reciprocal lattice point will be elongated along an axis perpendicular to the fiber axis and perpendicular to the surface of the lamella because of the small dimension in that direction. The next lamella of down helices will contribute its own interference region at each reciprocal lattice point, and the vectors for scattering from the two lamellae will add over the region of overlap of the interference regions. In this way scattering from successive lamellae of different thickness will lead to a sharpening of the diffraction spots at the reciprocal lattice points coupled with a general background intensity due to the overlap of the different sized interference regions. Thus we expect diffraction intensities to be calculable by adding the scattering vectors from the two types of lamellae using the appropriate phase factors and we expect a background intensity along the layer-line regions in the neighborhood of diffraction spots. Certainly the latter is observed in practice.

The question arises why the spacing between lamellae should be exactly the same as the lattice spacing within the lamellae and why the lateral shift between the up-helix lamellae and the down-helix lamellae should be exactly a half-lattice spacing. Actually there could be very slight differences between the lattice spacing and the spacing between lamellae and still the scattering vectors over several lamellae could approximately sum, provided each crystallite contains not very many lamellae. Calculation shows that small shifts in the spacing between lamellae and small shifts in half-lattice spacing between lamellae do not have a large effect on the structure factor calculations.

If the ω helices in poly(β-benzyl L-aspartate) are arranged in lamellae as we have suggested and since the ω-helix structure seems not to depend on whether it is derived from a left-handed α-helix structure or a right-handed structure there must be considerable molecular movement and atomic movement in the solid film at the high temperatures ($\sim$140°) needed to form the ω structure. As pointed out by Malcolm,[4] the change-over in helix sense which occurs for one helix sense of the unheated polymer when the ω-helix structure is derived from it need not involve a net rotation of a whole molecule about its axis, since if hydrogen bonds are broken locally on a helix a change of helix sense can occur by rotation about the α-carbon atom bonds. Malcolm suggested that such a breaking of hydrogen bonds and reforming of the reverse sense helix could propogate along the length of molecules.

However, the change in the molecular packing from the α forms of the polymer to the suggested lamella structure of the ω form indicate considerable molecular movements at the high temperatures, and large molecular movement is also shown in the formation of the ω form of poly[β-(*p*-chlorobenzyl) L-aspartate] with the work of Takeda *et al.*[17] Since the intermolecular interactions are clearly important in the formation of the ω structure, the big change in molecular packing must be integrally associated with the actual nucleation and growth of the phase change from the α to the ω form.

If molecules in an ω-helix pack parallel in a tetragonal lattice, there can be no reason for meridional reflections other than the 1.3-Å reflection on the fourth-layer line. Any distortion due to the packing of the molecules would just produce ω helices of different atomic coordinates and anyway the intermolecular interactions are believed to be important in stabilizing the ω structure in poly(β-benzyl L-aspartate). If one thinks of a down ω-helix pack isolated within a sizable group of up ω helices in a $P4_3$ structure it is clear that those residues of the up helices adjacent to the single down helix are in a different environment than they would be in an environment of up helices. It is therefore interactions between antiparallel helices which produce distortions from the ω-helix structure and which therefore produce the observed extra meridional reflections. No doubt in the lamella model the intramolecular interactions hold the side chains of the ω helices roughly rigidly in azimuth so that distortions due to intermolecular interactions are likely to be greatest in the helix axis direction, and such distortions would produce meridional reflections. The (001), (002) and (003) reflections in Plate 1A,B are fairly intense and since these would be due to interactions *between* the lamellae on our model, their presence would suggest that the lamellae are rather thin.

McGuire *et al.*[11] have shown that whereas an isolated molecule of $(BzAsp)_n$ is stable as the left-handed α helix in the solid state, intermolecular interactions between benzene rings and overlapped packing of the side chains of neighboring molecules result in the ω helix having the greatest stability. They calculate a structure for the ω helix which gives good agreement with the infrared data except that the benzene rings do not have the correct orientation with respect to the helix axis as indicated by infrared dichroism measurements. However, so far as we can tell the structure proposed by McGuire *et al.* does not agree with the diffraction measurements. The projection electron density map of Figure 5 shows extremely low electron-density regions half-way between molecules which strongly indicates that overlapped packing of the type suggested by McGuire *et al.* does not occur in the structure we studied. Structure factor calculations were made using the model of McGuire *et al.* for the case of a random distribution of parallel and antiparallel helices and for the case of a lamella model such as proposed in this paper. These calculations did not agree with the observed X-ray and electron diffraction data. It would be interesting to see if the calculations using the methods of McGuire *et al.* would lead to lower energy situations if intramolecular interactions between benzene rings were taken into account.

The position C for the benzene rings in the ω form of $(BzAsp)_n$ proposed by Happey *et al.*[12] would not take advantage of the considerable advantages obtained by stacking of the benzene rings so that they are in contact with a van der Waals thickness of 3–4 Å. It seems probably that at higher temperatures the benzene rings rotate between the two stable positions A and B to agree with their results and that at a low temperature they occupy the more stable of these two positions. As pointed out by Happey *et*

al.[12] the rotation of a benzene ring cannot be entirely independent of rotations in neighboring residues and no doubt this fact together with the packing problems for ω helices discussed above prevents an exact analysis of the diffraction data.

Acknowledgments. We are grateful to Dr. A. Elliott of King's College, London, for his constant interest and advice during this work and to Dr. B. R. Malcolm of Edinburgh University for helpful discussions. We are also indebted to colleagues in the X-ray diffraction group at Portsmouth Polytechnic for use of computer programs and to Professor H. A. Scheraga of Cornell University for kindly sending us information on the ω-helix structure proposed by McGuire *et al.*

Calculation of the Conformation of the Pentapeptide *cyclo*(Glycylglycylglycylprolylprolyl). III. Treatment of a Flexible Molecule[1]

Gregory C.-C. Niu, Nobuhiro Gō,[2] and Harold A. Scheraga*

Department of Chemistry, Cornell University, Ithaca, New York 14850.
Received September 22, 1972

ABSTRACT: In previous conformational energy calculations on this cyclic pentapeptide, the hard variables [bond lengths, bond angles, and dihedral angles around peptide bonds (ω's)] were kept constant; in this paper, the restriction of constancy of these variables is removed. Flexibility is introduced by assuming that a Urey–Bradley-type force field is applicable to the hard variables. Starting with the thirteen minimum-energy conformations (obtained previously in the rigid-molecule treatment), and using the conjugate gradient method, the total conformational energy was minimized in the extended space corresponding to the flexible-molecule treatment. Eight local minima were thus obtained, some of them arising from more than one (rigid molecule) initial conformation. In a strained molecule such as this one (*i.e.*, one with a few close interatomic contacts), energy barriers between local minima of the rigid-molecule treatment often disappear when the hard variables are allowed to vary. While the dihedral angles (φ's, ψ's, χ's) change very drastically from those of the initial conformations in many cases, the changes of bond lengths, bond angles, and ω's are within the range of X-ray crystallographic data.

In the first two papers[3,4] of this series, conformational energy calculations were carried out for the cyclic pentapeptide *cyclo*(Gly-Gly-Gly-Pro-Pro), which has eight single bonds in the backbone about which rotation can take place. The hard variables[5] [bond lengths, bond angles, and dihedral angles around the peptide bonds (ω's)] were maintained constant[3,4] (rigid molecule), and six of the backbone dihedral angles were computed as functions of the two (remaining) independent backbone dihedral angles. The complete energy surface of the rigid molecule was calculated, and thirteen local minima were located in that region of the energy surface which is within 100 kcal of the global minimum.[3] Using the assumption of small conformational fluctuations,[5] the statistical weights of the three lowest-energy local minima were computed[4] in terms of det **G** and det **F** (quantities that have been defined previously[5]), thereby providing information as to the most stable conformation of this cyclic pentapeptide (in the absence of solvation and crystalline forces).

The purpose of the present paper is to remove the restriction of constancy of the hard variables, and thereby obtain a more complete description of the cyclic pentapeptide; *i.e.*, every atom of the molecule is now allowed to move independently. The treatment of the molecule as a flexible one is the last step of a theoretical framework proposed earlier[5,6] for conformational energy calculations in general. In order to allow the hard variables to change, appropriate potential functions are required. By including such potential functions, together with those used[3] in the treatment of the rigid molecule, we may start from the conformations obtained in the rigid-molecule treatment and minimize the total conformational energy.[5,6] Thus, we require appropriate potential functions for treatment of the hard variables, and also a suitable energy-minimization procedure in order to carry out the computations for a flexible molecule.

In the rigid-molecule treatment, the problem of ring closure was a nontrivial one.[3] However, in the flexible-molecule treatment, no such problem arises since the potential functions for the hard variables serve to maintain the independently moving atoms in a closed ring.

As far as the potential functions are concerned, we may assume that the displacements of the hard variables from their equilibrium positions obey a simple harmonic law, with force constants obtained from infrared and thermodynamic data on simple molecules. While more work has to be done to be assured that force constants (determined in this way) can be used for more complicated molecules like *cyclo*(Gly_3Pro_2), we follow present practice,[7,8] and use them as a first approximation.

(1) This work was supported by research grants from the National Institute of General Medical Sciences of the National Institutes of Health, U. S. Public Health Service (GM-14312), from the National Science Foundation (GB-28469X1), and from Walter and George Todd.
(2) On leave of absence from the Department of Physics, Faculty of Science, University of Tokyo, Tokyo, Japan, 1967–1970, and the summer of 1971, and from the Department of Physics, Kyushu University, Fukuoka, Japan, the summer of 1972.
(3) N. Gō and H. A. Scheraga, *Macromolecules*, 3, 188 (1970) (hereafter referred to as paper I).
(4) N. Gō, P. N. Lewis, and H. A. Scheraga, *Macromolecules*, 3, 628 (1970) (hereafter referred to as paper II).
(5) N. Gō and H. A. Scheraga, *J. Chem. Phys.*, 51, 4751 (1969).
(6) H. A. Scheraga, *Chem. Rev.*, 71, 197 (1971).
(7) K. D. Gibson and H. A. Scheraga, *Biopolymers*, 4, 709 (1966).
(8) A. Warshel, M. Levitt and S. Lifson, *J. Mol. Spectrosc.*, 33, 84 (1970).